Progress reached? - Lifetime Prediction for UD-materials by using S-N curves, Kawai's Modified Fatigue Strength Ratio and Novel Haigh Diagrams

Ralf Cuntze
D-85229 Markt Indersdorf, Matthaeus-Guenther-Str. 32, Ralf_Cuntze@t-online.de;
formerly MAN Technologie AG, Augsburg, Germany,
now linked to Carbon Composites e.V. (CCeV), Augsburg, and CC-TUDALIT, Dresden

Summary:

Experience shows that multi-directional laminates, composed of endless fiber-reinforced UD laminas, statically designed to a design strain limit of $\varepsilon < 0.3\%$, do not fatigue. However, lightweight design requires a higher exertion of such materials.
The author presents a rigorous engineering-like method for fatigue life estimation which is equivalent stress-based on his WWFE-successful static 'Failure Mode Concept', the basis of his 'Mises-like' UD strength failure criteria set and that tool the damaging portions are calculated with.
The proposed method consists of: (1) Novel failure mode-based modeling of the varying operating stress state; (2) measurement and mapping of Master-S/N-curves for each activated failure mode (2 fiber and 3 matrix fracture failure modes); (3) determination of necessary other S/N curves within a single failure mode by employing Kawai's 'modified fatigue strength ratio' together with the obtained master curve of the specific failure mode; (4) generation of failure mode-linked Haigh diagrams which involve all S-N curves necessary for fatigue life estimation; (5) application of Miner's rule for the embedded lamina in order to accumulate the damaging portions.
The method will enable an effective and faster design development after the transfer from the embedded lamina to a general laminate will be validated. Special tests for embedded laminas together with multi-layered multi-directional laminates are required to capture the occurring in-situ effect.

1 Introduction and Objectives

System and concurrent engineering of the involved technical disciplines, analysis and simulation are recognized as key enablers to increase competitiveness. The thereby applied tools must give confidence to the designer [Cun16].
Composite components with very different matrices are increasingly used in primary load carrying structures in Aircraft, Automotive and Civil Engineering (CFR-polymer and -concrete), taking advantage of the increased structural strength and stiffness to weight ratios, corrosion resistance, or more innovative design capabilities. Increasing use requires a better understanding of the composite's behaviour under static, cyclic, and impact loading while experiencing various environments. *Fig.1* presents a look at the structural Design Verifications to be provided in order obtain Structural Integrity as precondition for product certification. Such a design may consider thick composite sections with large numbers of layers, there may exist regions of significant ply drop off, sandwich constructions and bonded joints, eventually also braided materials may be used. Therefore, design verification is very difficult and can often only be partly reliably solved by incorporating expensive structural tests.

Modern light-weight structures are the result of an optimisation compromise between all the product's functional requirements such as stiffness and strength, and of the operational requirements such as lifetime. Design driving are the material properties and the failure conditions for initiation of failure and final fracture of the usually relatively brittle behaving composite materials. The material addressed here is the transversely-isotropic UD lamina. Responsible for the goodness of the structure, designed under e.g. a minimum mass requirement, are a qualified analysis procedure, the input of reliable data involving the material properties, including the dimensioning load cases and the safety concept. Special task of the designer is the development of a so-called robust structure that does not essentially change its behaviour under the usual scatter of all the stochastic design parameters. When doing this the engineer must rely on the existence of qualified processes such as validated software,

analysis, tests and manufacturing as well as NDI procedures. And this must be considered under cyclic loading the more. Thereby, *What is failure?* is to define as an essential project-depending task.

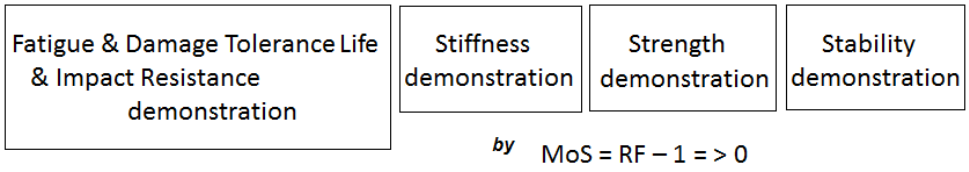

Fig.1: Necessary Design Verifications. Margin of Safety MoS, Reserve Factor RF

Failure is defined as: *The structural part does not fulfil its functional requirements*. Such failures are fiber failure FF, inter-fiber-failure IFF (matrix failure), leakage of a vessel, a deformation limit or a delamination size limit. The design driving failure modes must be fixed in each application! Traditionally, First-Ply-Failure FPF (nowadays often seen as onset of damaging or of failure) and Last-Ply-Failure LPF (final, usually sudden fracture occurs after last FF) are distinguished. Failure may be also a distinct degradation sum *D* as the result *of the accumulation of damaging portions under cyclic loadings.* In this context, Failure Assessment is mandatory which must include structure, laminate and lamina (ply). Thereby, it is to be discriminated between tolerable failure and final failure which might be a catastrophic one. For UD material all 5 failure modes FF1 (tension) and FF2 (compression), Inter-Fiber-Failure IFF1 (tension), IFF2 (Compression, kinking) and IFF3 (in-plane shear) with their degradation effects are taken into account. First-Ply-Failure including onset of delamination of a ply in thickness direction can be predicted by 3D UD strength criteria [Cun04, 13, 14, Puc02]. Of course, FF means final catastrophic failure. Dependent on the actual case the same may be valid for IFF2, whereas IFFI (lateral tension) and IFF3 (shear) behave more benign and residual strength and stiffness capacity remain after FPF. The grade of the criticality of a distinct failure needs to be assessed in each project application due to the active softening curve. Under monotonic loading at first diffuse and later discrete (localized) micro-damaging takes place. Under cyclic loading damaging is more diffuse than under static loading.

2 Structural Modeling Aspects

There are several possibilities to model a laminate. The first is to homogenize the constituents matrix and fiber to a transversely-isotropic lamina material. A second is to use laminate properties and a third to stay on the microscopic level of the constituents and bridge by meso-models to the lamina level.

Fatigue Design Analysis and Design Verification may be performed on different levels (1) *Structure*: forces and moments (e.g. pressure load of a tank); (2) *Cross-section*: section forces and section moments (beams, shell wall), and (3) *Material:* stresses in a material 'point' within the structure. In this case the first task is to transfer the loadings into stress states considering proportional and non-proportional stresses.

The structure's load-carrying capacity is mainly *locally* determined: in the critical material locations of undisturbed areas (plain areas etc.) by the local stress state; in disturbed areas like holes or at stress-raising stiffness jumps by a stress concentration (notch mechanics employed); and at delamination sites within a laminate by stress intensity affording the application of fracture mechanics. These stress situations are related to different strength quantities better termed resistances such as classical strength R , the notch strength, and the fracture toughness. Here, the material stress is addressed.

Generally, design analysis means investigation of the average behavior of the structural component. Therefore, average (typical) physical properties, including an average stress-strain curve with average values, are applied whereas in design verification of the chosen design statistically-based minimum and maximum properties are utilized. The use of average values ends up with a structural behavior that meets the real behavior best, namely with a 50% expectance value. This is also valid when validating fatigue models.

At present, usually a semi-probabilistic safety concept is applied in mechanical engineering for design verification: It employs: (1) a factor of safety *j* to increase the external loadings (e.g. *j*· Design Limit Load= *j*· DLL= Design Load DL); (2) takes statistically minimum values for the resistances (strength etc.) in order to further implement reliability into the structure.

Adequate UD strength failure criteria are necessary to compute the damaging portions: For UD-materials the World-Wide-Failure-Exercises-I and -II have tested all available strength criteria and sorted out the better ones. Cuntze's 3D Failure-Mode-Concept (the 'Mises' under the UD criteria) and

Puck's 3D Action Plane-Criteria could map the provided reliable test data best. About 30% of the data sets were not correct in the WWFE-II. Above 3D strength criteria are also capable of predicting onset-of failure in thickness direction. However, then lower strength values are used in thickness direction than in the lamina plane in order to simply consider the orthotropic material effect on top of the transversely-isotropic lamina material model and analysis. Practice desires macro-mechanical strength failure criteria but – as failure occurs at the constituent level - these criteria must reflect constituents' failures [Cun12].
There are many effects causing non-linearity such as Large deformations (geometry), large strains (material), change of fiber orientation, post-initial failure behaviour due to degradation (requiring the softening curve part), etc. Non-linearity significantly determines the cyclic damaging process.

3 Basics of the Cuntze's Fatigue Life Estimation Method

3.1 Mapping of S-N Curves and mode-linked Master Curve

The choice of the S-N model mainly depends on the fact whether an endurance limit for VHCF is given, and what should be mapped or not. An endurance limit should exist for FF1 of CFRP. As still mentioned, for brittle behaving materials it is physically reasonable to use the average strength (bar over) as maximum stress σ_{max} at N = 1. Possible mapping formulations are non-linear curves such as the Weibull-model and the Wearout-model, [VDI 2014], and linear models in the log-log diagram as used here. In *Fig.2*, exemplarily, the mapping result of of a small sample size FF1 test data of a CFRP material is collected. Since the test data set is for the stress ratio R = 0.1 (the measurement of R < = 0 is instability-endangered) it is the basic or the master FF1 S-N curve, with *R = stress ratio,* $\overline{R}$ = *average strength.* Considering the stochastic nature of the problem, it seems to be sufficient for

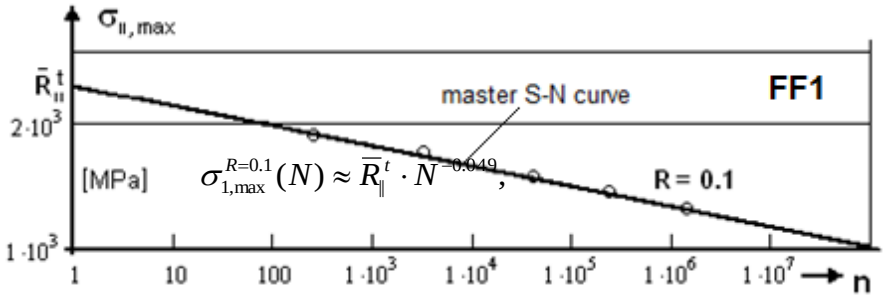

Fig.2: Modeling of the mode-representative measured master S-N curve [test data: Kawai].

engineering application to apply the model $\sigma_{\max}(N) = \overline{R} \cdot N^{c1}$.
How the determination of other mode-associated S-N curves beside the mode-governing master curves - necessary to predict lifetime – works will be depicted now.

A Fatigue-life-model that applies S/N curves needs many test data. In order to reduce this test effort, it would be very effective - to perform a lifetime prediction for a laminate on basis of an *in-situ master lamina S/N curve* for each single failure mode. Further S/N curves for the same failure mode, required in fatigue analysis, can be predicted from the master curve by utilizing the classical strain energy equality principle, applied for UD material in [Sho06, Cun09, Kaw04] or by employing Kawai's modified fatigue strength ratio (author prefers now Kawai's idea, it better predicts). This procedure enables the engineer during pre-dimensioning to build lifetime predictions for variable loading in tension, shear and compression on a cheaper and faster basis. There is some hope that at least for fiber-dominated laminates an embedded (in-situ) lamina fatigue design may replace the laminate design.
Note: Well-designed CFRP laminates show flat S-N curves.

3.2 Determination of other S-N Curves for FF1 on Basis of Kawai's Modified Fatigue Strength Ratio and of the Master Curve

Kawai first normalizes the fatigue strength σ_{max} by the static strength $R_{\parallel}^{t}$, which means the use of the material stressing effort (bar over is skipped here)

$$Eff^{\parallel\sigma} = \sigma_{max} / R_{\parallel}^{t} .$$

Eff corresponds to Kawai's ψ, termed *fatigue strength ratio.* Using the alternating stress σ_a and the mean stress σ_m the static failure condition above can be expressed as

$$Eff^{\parallel\sigma} = (\sigma_a + \sigma_m)/ R_{\parallel}^{t} \equiv \psi.$$

In the fracture case, meaning $\psi = 1 = 100\% \equiv Eff^{\|\sigma}$, this reads

$$\psi = 1 = \sigma_{max} / R_{\|}^{t} = (\sigma_a + \sigma_m) / R_{\|}^{t} \quad or \quad 1 = \sigma_a / (R_{\|}^{t} - \sigma_m).$$

Analogically to ψ, Kawai defines the also non-dimensional *modified fatigue strength ratio [Kaw04]*

$$\Psi = \sigma_a / (R_{\|}^{t} - \sigma_m) = 0.5 \cdot (1-R) \cdot \sigma_{max} / [R_{\|}^{t} - 0.5 \cdot (1+R) \cdot \sigma_{max}],$$

as a scalar quantity and thereby introduced the stress ratio *R*. Employing the formula above he normalizes the test data for different R-curves to a band of scattering test points. Fitting the course of test data Kawai obtains a Master Ψ-curve. Based on the chosen fit function for σ_{max} the S-N curves can be estimated by the resolved equation

$$\sigma_{max}(R) = (2 \cdot R_{\|}^{t} \cdot \Psi_{master}) / [\Psi_{master} - R + R \cdot \Psi_{master} + 1].$$

3.3 Fracture Failure Mode-related Discussion of Haigh Diagrams

A *Haigh diagram* involves all S-N curves necessary for fatigue life estimation. *Fig.3* displays as a simpler understandable isotropic case with its two fracture failure modes Normal Fracture NF under tension and Shear Fracture SF under compression. Viewing the diagram it can be recognized: The author describes Haigh diagrams failure mode-wise

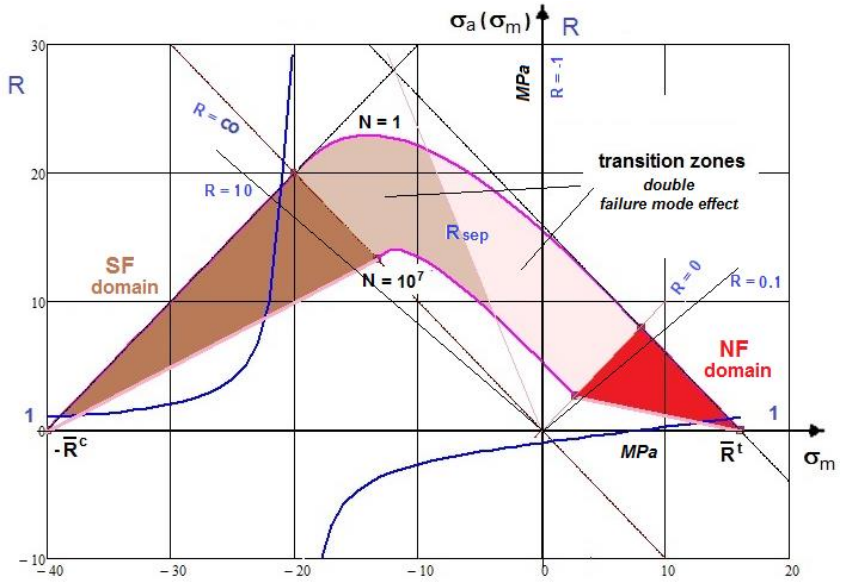

Fig. 3: Schematic Haigh diagram of a brittle behaving isotropic material experiencing two fracture failure types NF, SF and the course of the stress ratio R (σ_m). 50% average mapping of data. Strength $R^t = R_m$

Of highest concern is the course of constant fatigue life (CFL) curves especially in the transition zone between the mode-dominated domains at the left (negative) and right (1 > R > 0). In this zone, the CFL curve is the damaging result of two commonly active modes or a joint action of the two modes NF and SF takes place. The stress ratio *R = -1* delivers only some validating test points in the transition zone (similar to the joint action in the quasi-isotropic σ_2-σ_3-plane of the UD material). One should better measure the so-called (not well termed) critical stress ratio $R_{cr} = -R^c / R^t_{\ it} \equiv R_{sep}$ (better formulation as it is termed in [VDI2014]). The reason is, R_{sep} is more general than *R* = -1 (is a special case of an R_{trans} in the transition zone) which practically defines a separation line where maximum interaction takes place. For n > 10^4 the S-N curves of notched and 'plain' composites narrow. In the transition zone crack-closure effects occur.

In the UD case there exist 3 Haigh diagrams (2D): one for FF and two for IFF, IFF1 with IFF2, and further IFF3 for in-plane shear. Including IFF3, a 3D Haigh surface is obtained (see [Wei11, Gai16].

4 Fatigue and Damage Tolerance

4.1 Fatigue

The cyclic failure behavior of fiber reinforced plastic (FRP) composites is quite different from that of a ductile behaving metallic material. A general engineering-like method for the estimation of the life-time of high-performance UD-lamina material-based laminates does not yet exist [Koc16, Cun10]. A reliable method is highly desired, generally applicable to different laminas and laminates.

Essential for the lifetime analysis is the stress level: Low Cycle Fatigue LCF means high stressing, High Cycle Fatigue HCF means intermediate stressing and Very High cycle Fatigue VHCF low stressing and strains (for instance wind energy rotors, helicopter blades). Whether the damaging driver

remains the same from LCF until VHCF must be verified in each given case. The induced stress level at which fatigue failure occurs is lower than that for static loading. Initiation of fatigue failure is firstly diffuse and then becomes discrete at distinct material locations. It is affected by the environment such as by hygro-thermal effects in the case of polymer-matrix composites, i.e. Carbon Fiber Reinforced (CFRP) or Glass Fiber Reinforced Plastics (GFRP). For these types of composites experience proved, that if there are different fiber orientations given in the UD lamina-composed, multi-directional endless fiber-dominated laminate then a fatigue design verification is not necessary, presumed, a static 'fiber-dominated design' is performed for a limit design strain of $\varepsilon < 0.3\%$. However, future lightweight design requires a higher exertion of this material. CFRP Laminates may show an endurance limit.
Cyclic loadings are most often given by an operational loading spectrum which means a loss of the stress-time relationship.

For above composites, usually the same procedure is applied as for the more or less ductile behaving metals. However, physically much better fits a dedication to brittle behaving metals since these are more related to the usually brittle behaving composite materials. They also experience two different fracture failure modes under tension (normal fracture) and under compression (shear fracture). Ductile behaving metals, however, possess the same single yielding failure mode under tension and compression, whereby the so-called mean-stress effect is much smaller than in the brittle case.

4.2 Damage Tolerance

Damage Tolerance (not addressed further) is a property of a structure related to its ability to safely sustain a damage until repair can be affected. It builds upon the determination of damage growth and the establishment of inspection plans. It uses fracture mechanics to describe delamination crack growth under operational cyclic loading. A maintenance program must detect the damage and initiate the repair of accumulated and sudden accidental damage, applying reject and accept criteria for quality assurance. Fatigue consists of life until onset of damaging and further growth until damage initiation. In this context an engineer poses the questions: When does damaging start? How can one consider and compute the single micro-damaging portion (= Schädigung)? How can the single damaging portions be accumulated (for *fatigue verification*)? When do the accumulated damaging portions form a damage? When does such a damage (= Schaden, usually a delamination) become a critical size? Eventually, how is the damage growth (for *damage tolerance verification*) in the final phase of fatigue life in order to determine a part replacement time or fix inspection intervals?

5 Examples of Obtained Haigh Diagrams: Visualization and Discussion

5.1 The IFF3 Diagram τ_{21}, $\sigma_{eq}^{\perp\parallel}$

As the first Haigh diagram the FF3 diagram shall be provided. The static and thereby outer bounding curve is determined according to the interaction formula of the twofold acting static mode IFF3 or in other words the same mode acts twofold under *R* = -1. The determining *Eff* reads in the simple other case $I_{23\text{-}5} = 0$ with $Eff^{\perp\parallel} = \tau_{21} / R_{\perp\parallel}$. This is inserted into .

$$(Eff^{\perp\parallel})^m + (Eff^{\perp\parallel})^m = \left(\frac{-(\tau_{21m} - \tau_{21a}) + |\tau_{21m} - \tau_{21a}|)}{2 \cdot R_{\perp\parallel}} \right)^m + \left(\frac{(\tau_{21m} - \tau_{21a}) + |\tau_{21m} - \tau_{21a}|)}{2 \cdot R_{\perp\parallel}} \right)^m = 1 = 100\% \cdot$$

The absolute brackets are helpful when senseless negative *Effs* must be avoided.
For $N = 10^0 = 1$ the basic strength $R_{\perp\parallel}$ is used. It must be replaced for larger *N* by the *N*-associated residual strength σ_{max}(N), e.g. here exemplarily σ_{max} at $N = 10^5$ and at $N = 10^7$ cycles. These points are marked by a cross X on the S-N curves. If the S-N tests deliver just the standard test points for *R* = 0.1 and *R* = 10 these values are taken here as bounding values of the two modes, associated. Two S-N curves, *Fig.4,* were provided for the establishment of the IFF3 diagram, *Fig. 5*.

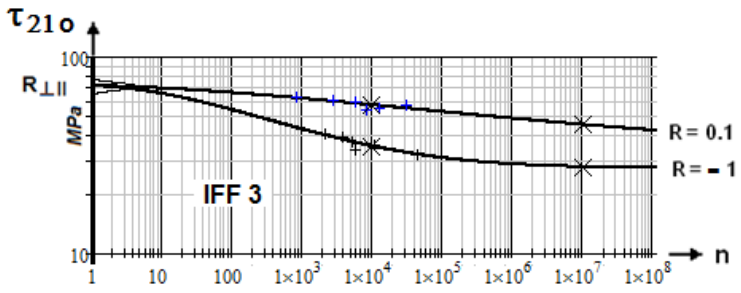

Fig.4: Log-log IFF3-linked S-N curves [data, courtesy C. Hahne]

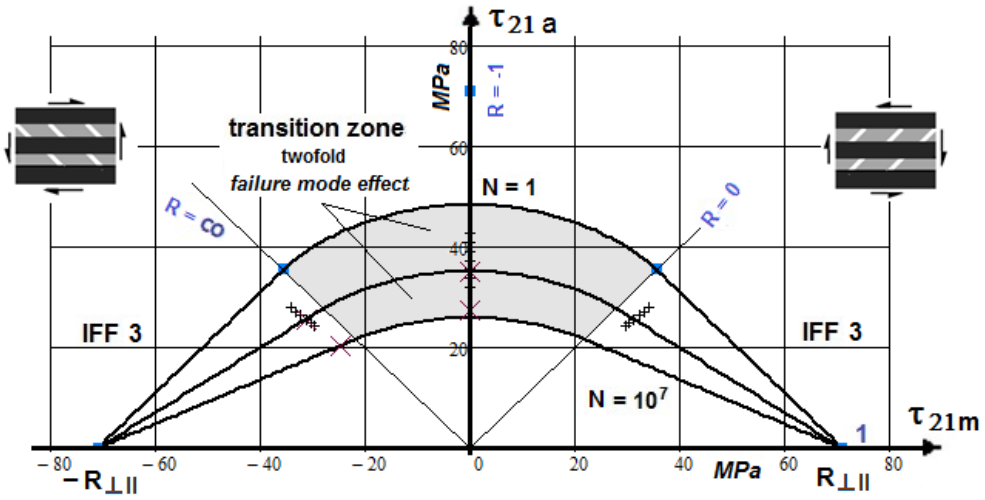

Fig.5: An IFF3 Haigh diagram, displaying a two-fold mode effect (a:= amplitude, m:= mean, N := number of fracture cycles, R := strength and R := $\sigma_{min}/\sigma_{max}$). Test data CF/EP, courtesy C. Hahne [Hah14], X = fix points

Notes: (1) Whereas here in the Haigh diagram the constant life curve part - within the transition zone - was the damaging result of a twofold active mode in the following diagrams it is the damaging result of similarly acting different modes. (2) Strength failure conditions (criteria) regularly describe just one occurrence of a failure mode linked to one failure mechanism. Therefore, a twofold acting mode, such as $\sigma_2 = \sigma_3$, with its higher damaging effect must be regarded on top.

5.2 The FF1-FF2 Diagram, σ_1, $\sigma_{eq}^{\|\sigma}$, $\sigma_{eq}^{\|\tau}$

Essential for the determination of FF-damaging is the provision of the FF1-FF2 Haigh diagram. The outer bounding curve is determined according to the interaction formula of the two modes FF1 (NF) and FF2 (similar to SF). This formula reads in the 2D case due to *Eff* = 1= 100%

$$(Eff^{\|\sigma})^m + (Eff^{\|\tau})^m = \left(\frac{-(\sigma_1 - \sigma_{1a}) + |\sigma_{1m} - \sigma_{1a}|)}{2 \cdot R_{\|}^{c}} \right)^m + \left(\frac{\sigma_{1m} + \sigma_{1a} + |\sigma_{1m} + \sigma_{1a}|)}{2 \cdot R_{\|}^{t}} \right)^m = 1.$$

It involves both, the two swelling zones and the transition zone as well, being the joint action domain of both the modes FF1 and FF2. Again, the absolute formulation keeps senseless negative *Effs* away. The CFL curves in *Fig.6* approximately map the associated points on the *R* = 0.5 curve. It must be noted that the test sample sizes were pretty small for a validation of the modeling method. As with the static case, also here, for general stress states the cyclic stresses in the Haigh diagrams are replaced by the associated equivalent stresses.

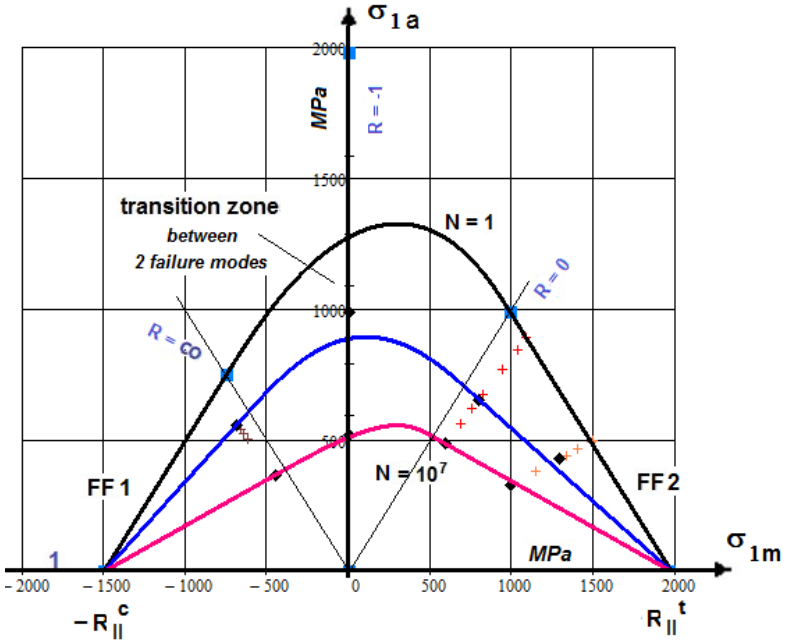

Fig. 6: An FF1-FF2 Haigh diagram, displaying the failure mode domains, transition zone, test data [Hah14]

5.3 The IFF1-IFF2 Diagram, σ_2, $\sigma_{eq}{}^{\perp\sigma}$, $\sigma_{eq}{}^{\perp\tau}$

Now, the IFF1-IFF2-Haigh diagram must be provided. This diagram describes fatigue in the quasi-isotropic plane of the transversely-isotropic UD material. The outer bounding curve is determined according to the interaction formula of the two modes IFF1 and IFF2. This formula reads, 2D case,

$$(Eff^{\perp\sigma})^m + (Eff^{\perp\tau})^m = \left(\frac{-(\sigma_{2m}-\sigma_{2a}) + |\sigma_{2m}-\sigma_{2a}|)}{2\cdot R_\perp{}^c}\right)^m + \left(\frac{\sigma_{2m}+\sigma_{2a}+|\sigma_{2m}+\sigma_{2a}|)}{2\cdot R_\perp{}^t}\right)^m = 1.$$

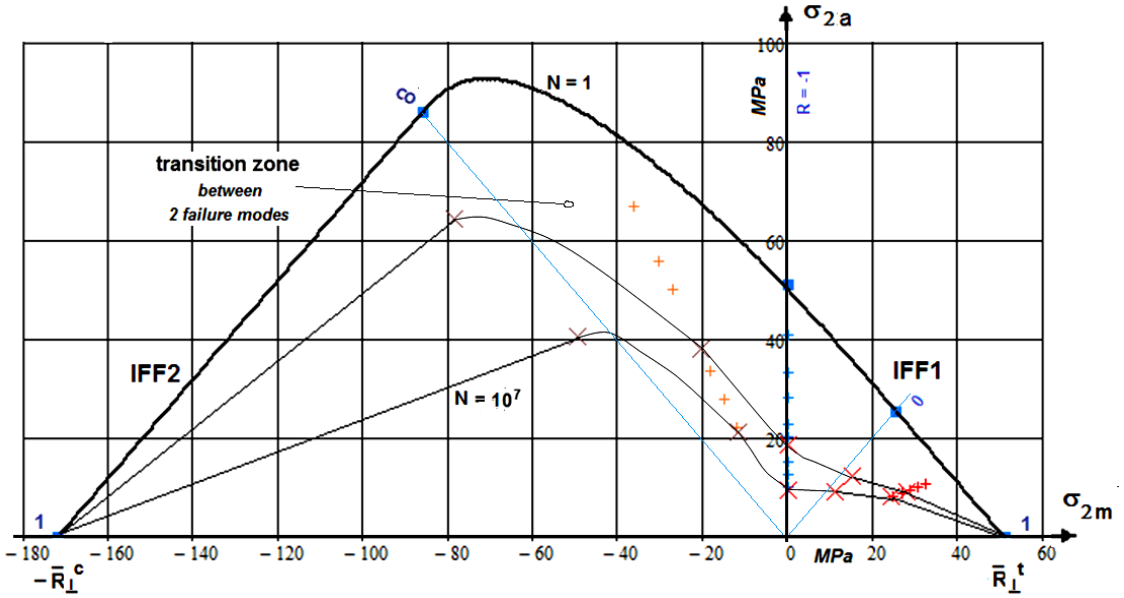

Fig.7: An IFF1-FF2 Haigh diagram, displaying the failure mode domains, transition zone, test data [Hah14] and the computed X-points as mapping fix points for the predicted CFL curves

Fig.7 represents the 'transversal' Haigh diagram. Unfortunately the complicated numerical computation of the CFL curve parts in the transition zone (interaction) did not yet work. Hence, these parts were mapped by hand.

6 Full Method with Numerical Application and Visualization

In the cyclic case the required lifetime could be principally demonstrated by

$$RF_{life} \approx \frac{\text{Predicted Lifetime}}{j_{life}\cdot \text{Design Limit Lifetime}} > 1.$$

After cyclic degradation caused by operational loading (< DLL), it must be demonstrated that the residual static strength is high enough to sustain Design Ultimate Load DUL (e.g. in spacecraft, DUL = j_{ult} · DLL). An important feature is the demonstration of the residual strength at DUL level for the replacement time procedure and at DLL level for the inspection method. For the designer, an important point in aircraft became the possibility to use a certification 'by tests' and 'by analysis supported by tests' which saves time and test costs.

Step 1: Modeling of loading cycles

For the sake of simplicity - for displaying the chosen load modeling idea in *Fig.8*- an isotropic brittle material is taken with a stress ratio *R* = -1. This was still proposed in 1996 by the author [Cun96]. The idea requires a *failure mode-linked apportionment of cyclic loading (better termed here stressing as the finally used derivative of loading.).* Of course, this idea must finally also lead to a mode-related accumulation of the damaging portions.

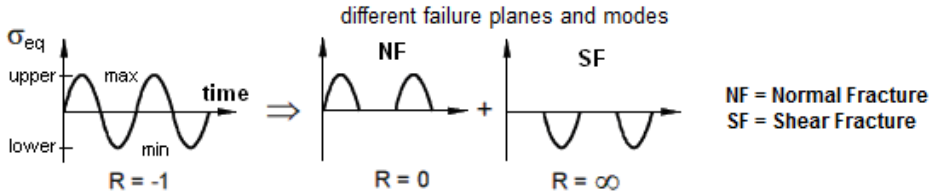

Fig. 8: Novel modeling of loading cycles

Step 2: Measurement and simple Modeling of master and to-be-predicted S-N curve (FF1)

Assumption: Mapping of the course of test data is possible by using the simple curve

$$\sigma_{\parallel,\,\max}^{master}(N) = \sigma_{\parallel,\,\max}^{R=0.1}(N) = \overline{R}_{\parallel}^{t} \cdot N^{c_{master}} \quad , \quad \sigma_{\parallel,\,\max}^{pred}(N) = \overline{R}_{\parallel}^{t} \cdot (N)^{c_{pred}} \quad .$$

This delivers *a straight line in the log-log diagram and* minimizes the calculation effort.

Step 3: S/N curve prediction by using M. Kawai's Modified Fatigue Strength Ratio

Assumption: Application of the strain energy equivalence principle is valid.

Further, the variable amplitude stress amplitudes of both the S-N curves were displayed together with the harsher constant amplitude loading

Step 4: Generation of failure mode-linked Haigh diagrams

These involve all S-N curves necessary for fatigue life estimation.

Step 5: Mode–associated accumulation of the damaging portions

Assumption: Palmgren–Miner's rule is applicable.

Accumulation of damaging portions $D_{\parallel}$, $D_{\perp}$, $D_{\perp\parallel}$ is performed by employing Palmgren-Miner's rule for the embedded lamina - cycle-wise, block-wise or otherwise -, however considering the stress-state-failure mode relationship. For the calculation of above damaging portions the 5 FMC-based static UD strength failure criteria can be applied. Presumption for an application of static criteria is: fracture failure modes are the same statically and cyclically.

Additional Step: Automatic generation of CFL curves in Haigh diagrams and IFF Surface

With a computed maximum curve (or min curve for *R* = 10), Step 3, the predicted S-N curve reads

$$\sigma_{\max}^{pred}(N) = \overline{R}_{\parallel} \cdot N^{c1pred} \quad , \quad \sigma_{\min}^{pred}(N) = R \cdot \sigma_{\max}^{pred}(N) \; .$$

Then, mean stress as well as amplitude stress can be calculated by using

$$\sigma_m{}^{pred}(N) = \frac{\sigma_{\max}^{pred}(N) + \sigma_{\min}^{pred}(N)}{2} \quad , \quad \sigma_a{}^{pred}(N) = \frac{\sigma_{\max}^{pred}(N) - \sigma_{\min}^{pred}(N)}{2} \; .$$

For the running variable stress ratio *R* and a fixed cycle number *N* continuous CFL-points ($\sigma_a(N)$, $\sigma_m(N)$) are given for each failure mode domain (here demonstrated for FF1). In this context: In [Wei] the complete test data set, that forms the full surface, is mapped by Tschebyscheff-Polynomials.

6.2 Visualisation for a FF Lamina Example

Eventually, in *Fig.10* a schematic application is presented. Of course, a maximum allowable damaging value D, the feasible D, is to be derived *experimentally based.* Example:

Static strengths: $\{\bar{R}\} = (2560,\ 1590,\ 73,\ 185,\ 90)^T\ MPa$,

S/N curves: $\sigma_{1,\max}^{R=0.5}(n) \approx \bar{R}_{\parallel}^{t} \cdot n^{-0.034}$, $\sigma_{\parallel,\ \max}^{R=0.1}(n) \approx \bar{R}_{\parallel}^{t} \cdot n^{-0.049}$,

Stresses: $\{\sigma\} = (\sigma_1, \sigma_2, \sigma_3, \tau_{23}, \tau_{31}, \tau_{21})^T$, $\{\sigma_{eq}^{mode}\} = \left(\sigma_{eq}^{\parallel\sigma},\ \sigma_{eq}^{\parallel\tau},\ \sigma_{eq}^{\perp\sigma},\ \sigma_{eq}^{\perp\tau},\ \sigma_{eq}^{\parallel\perp}\right)^T$.

Loadings: $n_3(R=0.1) = 0$

$n_1(R=0.1) = 100000\ cycles, \quad \sigma_1^{(1)} = 1250\ MPa, \quad N_1(R=0.1) = 2300000\ cycles,$

$n_2(R=0.1) = 1600\ cycles, \quad \sigma_1^{(2)} = 1500\ MPa, \quad N_2(R=0.1) = 55000\ cycles,$

$n_4(R=10) = 6000\ cycles, \quad \sigma_1^{(4)} = -1150\ MPa, \quad N_4(R=10) = 50000\ cycles,$

$n_5(R=0.5) = 600000\ cycles, \quad \sigma_1^{(5)} = 1550\ MPa, \quad N_5(R=0.5) = 2600000\ cycles.$

$D = \sum n_i/N_i) = 100000/2300000 + 1600/55000 + 6000/5000 + 600000/2.600000 = 0.43.$

$MoS = (D_{feasible} / D) / (j_{Life} \cdot D) - 1 = [(0.8/0.43) / (3 \cdot 0.43)] - 1 = 0.4 > 0.$

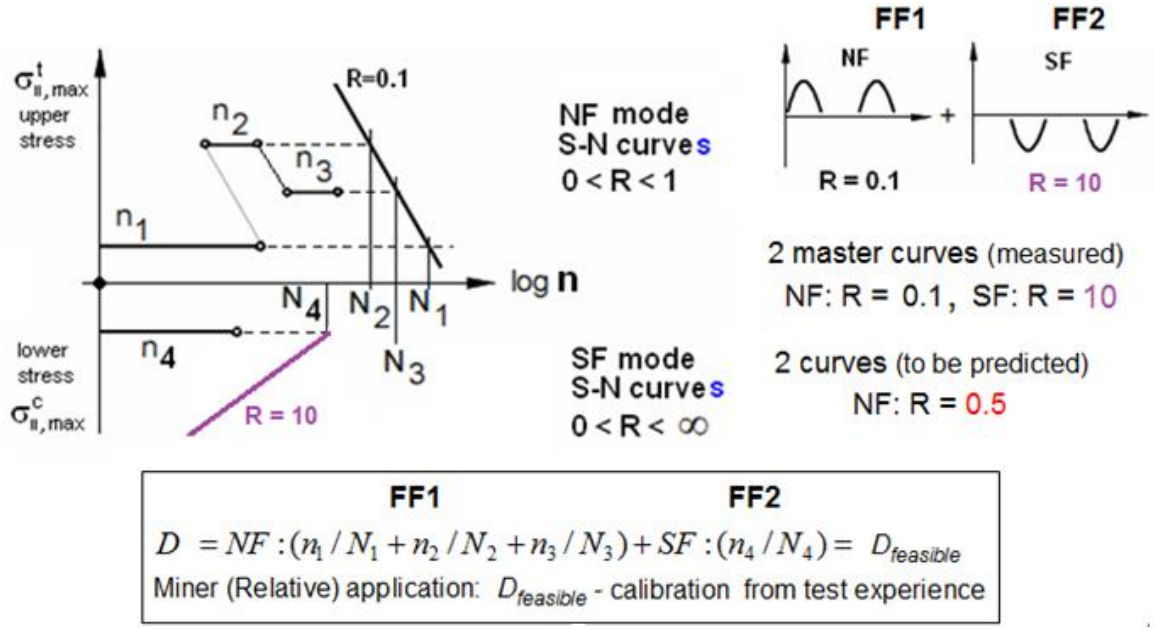

Fig. 10: Schematic application of the method for the two FF modes

Note: During manufacturing of composite parts residual stresses from curing and mounting may occur. An effect caused may be warping or a spring-in. In the case of filling, compaction, curing and consolidation process-simulation delivers essential input for the structural analyses during design dimensioning. Matrix nesting and voids may be also generated. Since fiber orientation is essential for stiffness and strength the manufacturing process must be qualified and non-acceptable draping orientation and undulation minimized.

Conclusions

Fatigue pre-dimensioning is possible: for 'well-designed', UD laminas-composed laminates by lamina dedicated FF- and IFF-linked, mode-representative S-N curves derived from sub-laminate test specimens, which capture the in-situ effect. Initial failure depends on the cycles-dependent shrinking of the IFF body determined by the degrading residual strength. The presented method consists of

1) Failure mode-linked load modelling and damaging accumulation (Miner)
2) Measurement of a minimum number of Master S-N curves
3) Prediction of other necessary *mode S-N curves* on basis of the master curve by the use of *strain energy equivalence*
4) Accumulation of damaging portions depends on cycles-linked shrinking of failure surface. In-situ-effect consideration by deformation controlled testing.
5) No classical mean stress correction needed.

What needs to be further investigated?

- How essential mode interaction damaging really might be and how the effect of loading sequence accounts for?
- What could be done if data in the transition zone are not available?
- Determination of $D_{feasible}$
- Effects of the negative notching a neighbor-lamina are to be seen in balance with the positive 'healing' effect due to redundant behavior when being embedded
- Applicability for further materials except the non-crimped fabrics NCF.

Literature *found under* **https://www.carbon-connected.de/Group/CCeV.Fachinformationen/Mitglieder**

[Cun04] Cuntze R.: *The Predictive Capability of Failure Mode Concept-based Strength Criteria for Multidirectional Laminates*. WWFE-I, Part B, Comp. Science and Technology 64 (2004), 487-516

[Cun10] Cuntze R.: *Failure Mode-based Lifetime Prediction of Brittle behaving UD Laminas-composed Laminates*. NAFEMS Seminar Wiesbaden 2010, Nov. 10 – 11. Conference publication. 10 pages

[Cun13] Cuntze R.: *Comparison between Experimental and Theoretical Results using Cuntze's 'Failure Mode Concept' model for Composites under Triaxial Loadings - Part B of the WWFE-II*. Journal of Composite Materials, Vol.47 (2013), 893-924

[Cun14] Cuntze R.: *The World-Wide-Failure-Exercises-I and –II for UD-materials – valuable attempts to validate failure theories on basis of more or less applicable test data*. SSMET 2014, Braunschweig, April 1 – 4, 2014, conference handbook

[Cun16] Cuntze R.: *Introduction to the Workshop - from Design Dimensioning via Design Verification to Product Certification*. Experience Composites 16 (EC16), September 21 – 23, 2016, Augsburg. Extended Abstract in Symposium Abstracts. 10 pages

[Gai16] Gaier C., Dannbauer H., Maier J. and Pinter G.: *Eine Software-basierte Methode zur Betriebsfestigkeitsanalyse von Strukturbauteilen aus CFK*. CCeV-Austria, AG Engineering, Meeting St. Martin im Innkreis, Sept.8. Magna-Powertrain, Engineering center Steyr

[Hah15] Hahne C.: *Zur Festigkeitsbewertung von Strukturbauteilen aus Kohlenstofffaser-Kunststoff-Verbunden unter PKW-Betriebslasten*. Shaker Verlag, Dissertation 2015, TU-Darmstadt, Schriftenreihe Konstruktiver Leichtbau mit Faser-Kunststoff-Verbunden, Herausgeber Prof. Dr.-Ing. Helmut Schürmann

[HSB] German Aeronautical Technical Handbook *'Handbuch für Strukturberechnung'*, issued by Industrie-Ausschuss-Struktur-Berechnungsunterlagen. TIB Hannover

[Kad13] Kaddour A. and Hinton M.: *Maturity of 3D failure criteria for fibre-reinforced composites: Comparison between theories and experiments*. Part B of WWFE-II, J. Compos. Mater. 47 (6-7) (2013) 925–966.

[Kaw04] Kawai M.: *A phenomenological model for off-axis fatigue behaviour of uni-directional polymer matrix composites under different stress ratios*. Composites Part A 35 (2004), 955-963

[Koc16] Koch I., Horst P. and Gude M.: *Fatigue of Composites – The state of the art*. EC16 symposium abstracts

[Pet16] Petersen E., Cuntze R. and Huehne C.: *Experimental Determination of Material Parameters in Cuntze's Failure-Mode-Concept -based UD Strength Failure Conditions.* Composite Science and Technology 134, (2016), 12-25

[Puc02] Puck A. and Schürmann H.: *Failure Analysis of FRP Laminates by Means of Physically based Phenomenological Models.* Composites Science and Technology 62 (2002), 1633-1662

[Sho06] Shokrieh M.M. and Tahery-Behroz F.: *A unified fatigue model based on energy method.* Composite Structures 75 (2006), 444-450

[Vas10] Vassilopoulos A.P.: *Fatigue life prediction composites and composites structures*. Elsevier Woodhead Publishing, 576 pages

[VDI2014] VDI 2014: German Guideline, Sheet 3 *Development of Fibre-Reinforced Plastic Components, Analysis*. Beuth Verlag, 2006. (in German and English, author was convenor)

[Wei11] Weinert A. and Gergely P.: *Fatigue Strength Surface: basis for structural analysis under dynamic loads*. CEAS Aeronautical Journal 2011, Vol.2, Issue 1, 243-252